RSC Advances

PAPER

View Article Online
View Journal | View Issue

Cite this: *RSC Adv.*, 2020, **10**, 32103

Elaborating piperazinyl-furopyrimidine based scaffolds as phosphoinositol-3-kinase enzyme alpha (PI3Kα) inhibitors to combat pancreatic cancer†

Mai A. Mansour, *[a] Deena S. Lasheen,[b] Hatem M. Gaber[c] and Khaled A. M. Abouzid *[bd]

Phosphoinositol-3-kinase enzyme (PI3K) plays a crucial role in driving oncogenic growth in various mammalian cells, particularly pancreatic cells. In the current study a series of novel furo[2,3-*d*]pyrimidine based-compounds were designed and synthesized as potential PI3K-α inhibitors. In accordance to the structure–activity relationship (SAR) studies of known PI3K-α inhibitors, different linkers including amide, urea and ether were attached to a piperazinyl furo[2,3-*d*]pyrimidine core. The synthesized compounds that revealed moderate PI3K-α inhibitory activity were tested for their anti-proliferative activities against pancreatic carcinoma on the PANC-1 cell line. Compounds **7b** and **8a** showed the highest anti-proliferative activity with IC_{50} values of 4.5 μM and 6 μM, respectively and relatively, the best *in vitro* PI3K inhibition ability within the newly synthesized compounds. Additionally, all the newly synthesized final compounds were tested on 60 human cancer cell lines. A docking study was carried out on the PI3K-α active site showing a comparable binding mode to that of FDA approved PI3K-α inhibitors. These newly discovered lipid kinase inhibitors could be considered as potential candidates for the development of new targeted anticancer agents.

Received 23rd July 2020
Accepted 21st August 2020

DOI: 10.1039/d0ra06428a

rsc.li/rsc-advances

Introduction

PI3K belongs to the lipid kinase family, responsible for phosphorylating the 3′-position (–OH) moiety of the inositol ring, yielding phosphatidylinositol-3,4,5-trisphosphate (PIP3), a messenger that in turn activates another serine–threonine protein kinase B (AKT) and the cellular messenger, mTOR.[1] This family is divided into three main classes (class I, II and III) based on their different structures and substrate specificities. Class I, our subject of concern, contains four different isoforms, that possess diverse catalytic p110 and regulatory subunits.[2] Stimulated by Tyr kinase, G protein-coupled receptors and Ras, class I PI3Ks use phosphatidylinositol-4,5-bisphosphate as their substrate and form a complex with a regulatory subunit, either a p85 isoform (for p110α, p110β and p110δ) or p101 or p87 (for p110γ).[3]

Dysregulation in the PI3K pathway is associated with many types of cancer due to its role in various cellular processes, including cell survival, proliferation and differentiation.[4–6] In pancreatic malignancies, separate studies showed that mutations in the K-ras gene occurred in the majority of pancreatic ductal adenocarcinomas (PDAC).[7] This oncogenic process causes the over-activation of the PI3K pathway,[4] particularly the catalytic subunit p110α of the PI3K-α isoform, which contributes to the super-activation of K-ras in the newly formed pancreatic ductal preneoplastic lesions.[8] Inactivating this single isoform ceased the irreversible transition of exocrine acinar cells into pancreatic preneoplastic ductal lesions.[9] Not to mention that, the downstream effector, AKT2, an oncogene encoding the protein kinase B, has also been found to be amplified in many pancreatic carcinomas,[10] making AKT activate in approximately (59%) of the pancreatic cancers.[11]

In the meantime, pancreatic cancer represents the seventh leading cause of cancer associated death, world widely,[12] and expected to be the second cause in the developed world by 2030.[13] This can be attributable to its low 5 year relative survival rate (9%) and poor prognosis.[14] However, PDAC, the most common malignancy of all pancreatic cancers (90%)[15] has surgical resection as the only recent chance for cure and prolonged survival.[16] Gemcitabine[17] and other aggressive chemotherapeutic combinations such as, FOLFIRINOX (folinic acid, 5-

[a]*Pharmaceutical Chemistry Department, Faculty of Pharmacy, Badr University in Cairo, Egypt. E-mail: maiali92@yahoo.com*
[b]*Pharmaceutical Chemistry Department, Faculty of Pharmacy, Ain Shams University, Abbassia, Cairo 11566, Egypt. E-mail: khaled.abouzid@pharma.asu.edu.eg*
[c]*National Organization for Drug Control and Research, Egypt*
[d]*Department of Organic and Medicinal Chemistry, Faculty of Pharmacy, University of Sadat City, Sadat City, Menoufia, Egypt*

† Electronic supplementary information (ESI) available. See DOI: 10.1039/d0ra06428a

fluorouracil [5-FU], irinotecan, oxaliplatin), albumin-bound paclitaxel (nab-paclitaxel) plus gemcitabine[18] delivered another intolerable protocol of treatment,[19] which revealed chemoresistance within weeks of treatment initiation.[20]

To improve treatment responses, targeting key regulators involved in the aberrant PI3K signaling pathway in PDAC has been implemented in clinical trials. Potent pan-class I PI3K inhibitor such as Copanlisib (**I**), Buparlisib (**II**), and ZSTK474 (**III**) as well as the FDA approved selective PI3K-α inhibitor, Alpelisib,[21] have been incorporated in a recent ongoing clinical study[22] (Fig. 1).

Upon exploring literature surveys and previously reported SAR studies as well as binding interactions of known potent PI3Kinase-α inhibitors, such as binding modes of Alpelisib (PDB code 4JPS)[23] and the ester-containing imidazopyridine HS-173 (IC_{50} = 0.8 nM)[24] (**V**), which as well as established potent anti-tumor efficacy *in vivo* xenograft and orthotopic pancreatic tumor models,[25] revealed three essential pharmacophoric features in a triangle arrangement.[26] (1) A hinge binder (HB) that interacts through the formation of the essential hydrogen bond with the backbone valine residue at the hinge region (Val851);[23] (2) an affinity pocket binder (APB) that fits into the cavity with possible hydrogen bonding to the catalytic lysine residue (Lys802, Tyr836, Ile932, Ile848, Ile800, Asp933, Pro778 and Met772);[23,27] (3) ribose pocket binder (RPB), a lipophilic group, that extends into the ribose binding pocket of ATP, also called region 1, made of 8 amino acids (Arg852–Gln859) maintaining isoform specificity.[28,29] In this study, we designed and synthesized a series of novel potential furopyrimidines targeting pancreatic cancer *via* the PI3K-α inhibition based on mimicking the purine portion of adenosine-5′-triphosphate (ATP)[30] providing binding to the hinge region of the kinase by hydrogen bonds with the backbone amino acids.

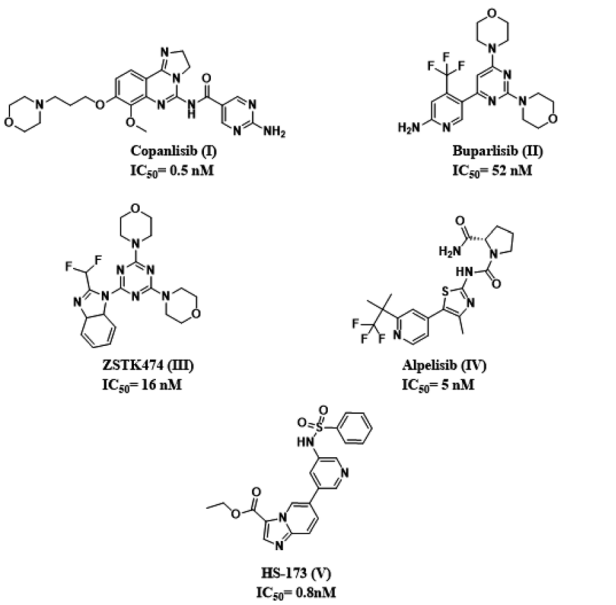

Fig. 1 Chemical structures of PI3K-α inhibitors used as clinical candidates in pancreatic cancer treatment with their corresponding IC_{50} against PI3K-α.

In order to design novel analogues and clarify the structure–activity relationships, we suggested the following modifications on the potent inhibitor HS-173 (**V**). The imidazopyridine heterocyclic ring forming the key hinge region hydrogen bond to the backbone-NH of Val851 through the nitrogen of imidazole the moiety was replaced with the fused furo[2,3-*d*]pyrimidine ring, aiming to form such interaction through hydrogen bonding *via* the oxygen atom of the furan ring. Whereas, the ester group attached to C3 was preserved to occupy the ribose pocket. A flexible aliphatic piperazine moiety was attached at position 4, due to its expected anti-tumor[31] and kinase inhibitory activity.[32,33] Besides, for better enzymatic and cellular potency, various amide and urea moieties were introduced to our target compounds aiming to provide the key interaction with the Lys802 amino acid in the catalytic region as observed in PKI402 (**VI**) and its triazolopyrimidines series, where the amides proceeded as a solubilizing group (Fig. 2).[34]

Results and discussion

Chemistry

The synthetic pathways for preparation of the target compounds were outlined in Schemes 1 and 2. In Scheme 1, the synthesis of furo[2,3-*d*]pyrimidine target compounds was started *via* the preparation of ethyl 5-amino-4-cyano-2-methylfuran-3-carboxylate (**1**) through reacting ethyl 2-chloroacetoacetate with malononitrile in sodium ethoxide following to the reported method.[35] Cyclization of compound (**1**) was afforded *via* its reflux with formic acid and acetic anhydride for 48 hours[36] to

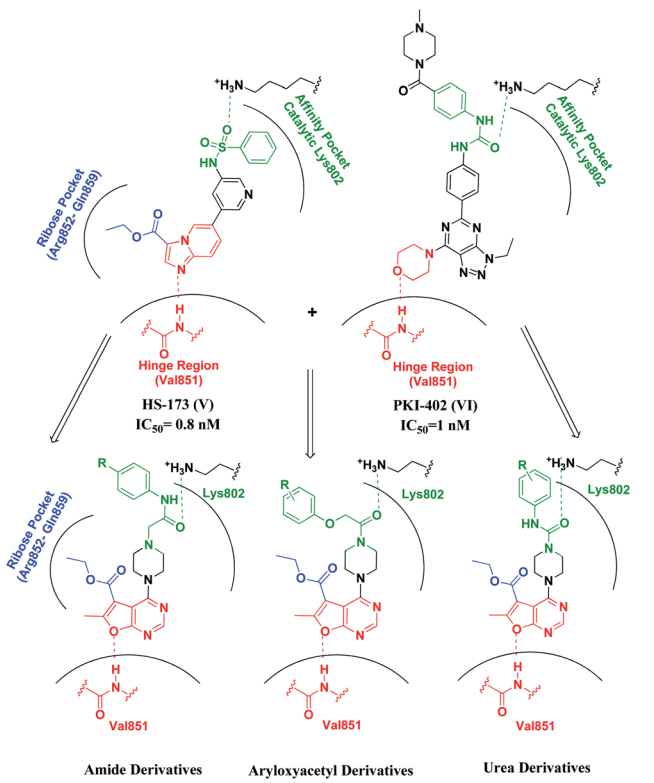

Fig. 2 Schematic illustration of the proposed scaffolds.

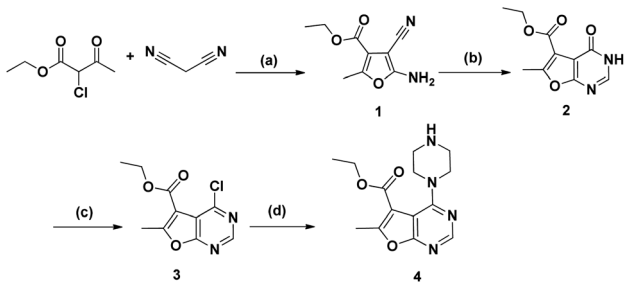

Scheme 1 Reagents and conditions: (a) NaOEt, rt, 6 h, 77%; (b) HCOOH, acetic anhydride, reflux, 48 h, 80%; (c) $POCL_3$, reflux, 3 h, 79%; (d) anhydrous piperazine, *i*-PrOH, reflux, 7 h, 60%.

yield the cyclized furo[2,3-*d*]pyrimidinone derivative (**2**). Afterwards, chlorination of the cyclized derivative (**2**) was achieved by reflux in phosphorus oxychloride, followed by coupling with anhydrous piperazine in isopropanol to attain the key intermediate (**4**)[37] Scheme 1.

The synthesis of the final compounds (**5a–d**) involved nucleophilic attack of the intermediate **4** on respective 2-chlorophenyl acetamide derivatives.[38] Whereas, according to Scheme 2, the synthesis of aryloxyacetyl derivatives, initially involved reacting chloroacetyl chloride with **4**, to afford the intermediate **6**, followed by Williamson's reaction with the appropriate phenols to achieve the compounds entitled (**7a–d**).[39] Finally, urea derivatives were afforded by nucleophilic addition of intermediate **4** to isocyanate and isothiocyanate derivatives, performed in chloroform at room temperature (Scheme 2).[40]

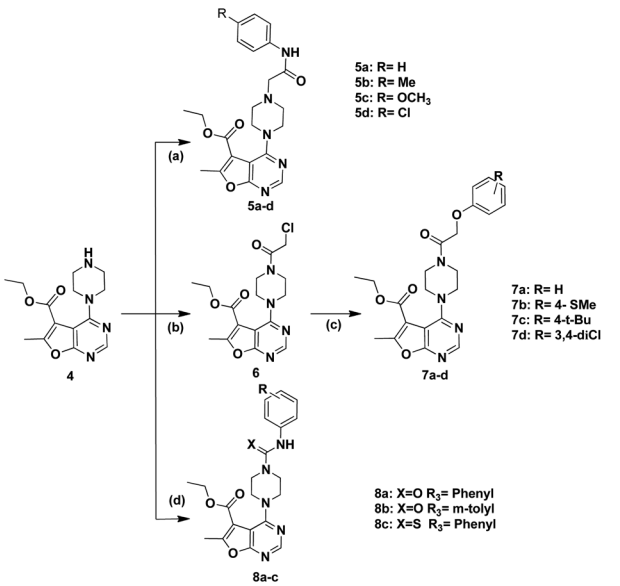

Scheme 2 Reagents and conditions: (a) appropriate 2-chlorophenyl acetamide derivatives, K_2CO_3, KI, acetone, reflux, 30–36 h, appropriate 2-chloro-*N*-phenylacetamide derivative; (b) chloroacetyl chloride, TEA, rt, 6 h; (c) appropriate phenol derivative, K_2CO_3, KI, acetone, reflux, 30 h, appropriate phenol derivative; (d) appropriate isocyanate and isothiocyanate derivatives, $CHCl_3$, 3–6 h, appropriate isocyanate and isothiocyanate derivatives.

Biological evaluation

***In vitro* PI3K-α activity at a single dose of 10 μM.** A single dose of 10 μM concentration of the designed compounds was used to evaluate their PI3K-α inhibitory activity using an Alexa Fluor™ 647 labeled ADP tracer, detecting the reduction in the amount of ADP formed in the presence of an inhibitor, by the kinase reaction. As shown in Table 1, the test compounds were able to moderately inhibit the PI3K-α isoform. PI-103 was used as a positive control.

At this concentration, the piperazinyl furo[2,3-*d*]pyrimidine-5-carboxylate derivatives (**7a**, **7b**) incorporating the aryloxyacetyl moiety and (**8a**, **8b**, **8c**) incorporating the substituted arylurea/thiourea moiety attached to the parent scaffold, revealed the moderate inhibition between (51–69%) against the PI3K-α kinase activity.

Upon investigating the structure–activity relationship among the newly synthesized furo[2,3-*d*]pyrimidines, the phenyl acetamide derivatives (**5a–d**) showed weak inhibitory activity (11–28%). The unsubstituted derivative (**5a**) relatively exhibited the weakest inhibitory activity; while final compounds (**5b–d**) having lipophilic substituents presented relative higher inhibition.

A significant increase in enzymatic inhibition was revealed in the 6-methylfuro[2,3-*d*]pyrimidines series (**7a–7d**) bearing the aryloxyacetyl moiety which is most probably attributed to the formation of the essential H-bond with the catalytic Lys802, which was proved to possess a crucial role in the phosphor transfer reaction and inhibitory activity.[41] Furthermore, it seemed that such linker permits more free movement of the

Table 1 Percent inhibition of PI3K-α enzymatic activity achieved by the designed compounds assessed at 10 μM

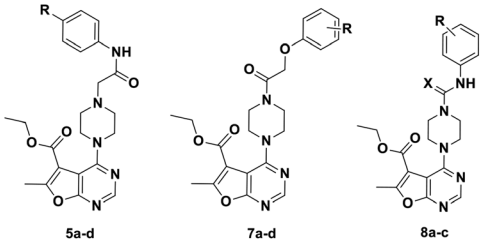

Cpd ID	X	R	% PI3K-α inhibition
5a	—	H	11
5b	—	CH_3	16
5c	—	OCH_3	20
5d	—	Cl	28
7a	—	4-H	53
7b	—	4-SCH_3	**59**
7c	—	4-*tert* Butyl	25
7d	—	3,4-DiCl	45
8a	O	H	**69**
8b	O	3-CH_3	51
8c	S	H	51
PI-103	—	—	100

terminal aromatic ring that extends to occupy the affinity pocket. The unsubstituted and thiomethyl derivative (**7a**, **7b**) showed best inhibition percentage within the series. However, incorporating a bulky *tert* butyl substituent at the terminal phenyl ring generally reduced the inhibitory activity. It can be postulated that the addition of bulky substituents hindered the aryloxyacetyl derivatives from fitting within the affinity pocket.

Upon the incorporation of the arylurea or thioarylurea linkers with the key intermediate, in final derivatives (**8a–c**), moderate enzyme inhibition was conserved as the free movement of the terminal aromatic ring is quite maintained, with a noteworthy increase in the inhibitory activity by the unsubstituted urea derivative (**8a**) that reached 69%.

***In vitro* PANC-1 anti-proliferative assay.** PANC-1 cell line is a primary tumor cell line currently used as *in vitro* models to study the carcinogenesis of pancreatic ductal adenocarcinoma.[42] Six compounds, with the PI3K-α percentage inhibition 45–69% were selected to be tested for their ability to inhibit PANC-1 cell line proliferation *in vitro*, using paclitaxel as a positive control. The results are illustrated in the (Table 2). Compounds (**7b**) and (**8a**) manifested moderate ability to inhibit PANC-1 cell line proliferation with IC_{50} values of 4.5 μM and 6 μM respectively, compared to paclitaxel 0.008 μM. These findings support our initial findings that these compounds possess a potential cytotoxicity on PANC-1 cells overexpressing PI3K alpha without noticeable cytotoxicity on the rest of cancer cell line panels (ESI†).

***In vitro* anti-proliferative activity assay against NCI 60-cell line panel.** All of the designed compounds were selected by the Developmental Therapeutics Program (DTP) of the National Cancer Institute (NCI), division of cancer treatment and diagnosis, NIH, Bethesda, Maryland, USA (https://www.dtp.nci.nih.gov). Utilizing 60 different human tumor cell lines, representing leukemia, melanoma, lung, colon, brain, ovary, kidney, prostate and breast cancers,[43] compounds were tested at initial single dose 10 μM inhibition percent assay. Upon analysis of the NCI-60 results, all of the compounds showed weak activity against most of the screened cell lines. The poor anti-proliferative activity exhibited by these derivatives may be accredited to the lack of activity against other kinases as PI3K-alpha is not highly expressed in these cell lines, thus it can be suggested that these compounds investigated by NCI may enjoy good selectivity profiles.

Table 2 The IC_{50} values of selected target compounds and paclitaxel on PANC-1 cell line

PANC-1 cancer cell line	
Cpd ID	IC_{50} μM
7a	10.70 ± 0.55
7b	4.50 ± 0.72
7d	10.20 ± 0.90
8a	6.00 ± 0.41
8b	9.98 ± 0.66
8c	17.00 ± 0.85
Paclitaxel	0.008 ± 0.23

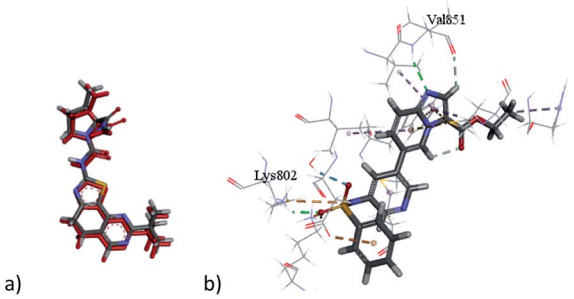

Fig. 3 (a) The alignment between the co-crystallized bioactive conformer (VII) (red) and the pose of the same compound retrieved from docking at PI3K-α binding site using CDOCKER. (b) Retrieved docking pose of the HS-173 (V) showing the same key interactions as reported.

Yet, compound **7c** was able to show the best mean inhibition within the furopyrimidine final compounds, with a value of 21.54%; however it displayed low PI3K-alpha inhibition 25%, indicating its possible activity against other kinases. A significant growth inhibition was achieved against the renal UO-31 cancer cell line with a value of 51.97%.

Molecular modelling

Docking study. CDOCKER protocol was performed for this docking study, using in Accelrys Discovery Studio® 2.5 software to achieve an overview into the SAR of the designed compounds, and to understand the results obtained by the biological evaluation on the basis of the ligand–protein interactions. The X-ray crystal structure of PI3K-α complexed with the selective inhibitor (**VII**) was obtained (PDB: 4ZOP). For the validation of the CDOCKER protocol, and its predictability of the correct poses,

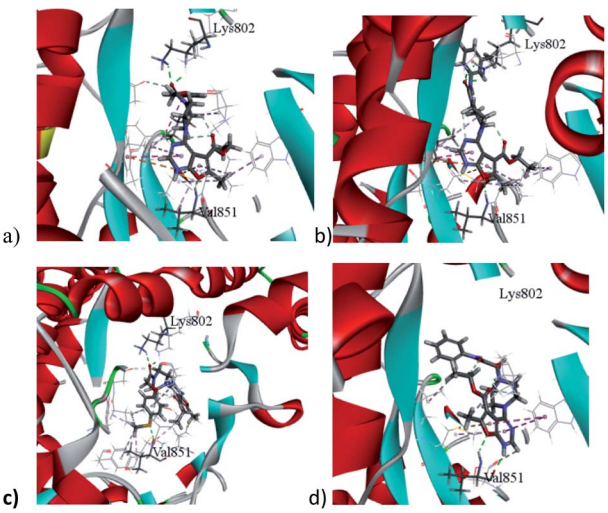

Fig. 4 (a–d) Docking poses of the target compounds (**7a**, **8b**, **7b**, **5a**) to the ATP binding pocket of PI3K-α. (a and b) Docking poses of (**7a** and **8b**) established the same key interactions as the lead compound; (c) docking pose of **7b**, established the same key interactions with different orientation. (d) Docking pose of (**5a**) missing one key interaction with Lys802 residue.

Table 3 *In silico* predictive ADME parameters calculated

Cpd ID	[a]A log P98	[b]Aqueous solubility level	[c]PSA_2D	[d]Intestinal absorption level	[e]BBB level
HS-173	2.934	2	88.702	0	3
5a	2.059	3	98.123	0	3
5b	2.545	2	98.123	0	3
5c	2.042	3	107.053	0	3
5d	2.723	2	98.123	0	3
7a	2.181	3	94.243	0	3
7b	2.723	3	94.243	0	3
7c	3.582	2	94.243	0	3
7d	3.51	2	94.243	0	3
8a	2.254	3	98.123	0	3
8b	2.74	2	98.123	0	3
8c	2.117	2	68.012	0	3

[a] Lipophilicity descriptor. [b] Aqueous solubility level; 4 = optimal, 3 = good, 2 = low solubility, 1 = very low but soluble, 0 = extremely low. [c] Polar surface area; compounds must have log *p* value not greater than 5.0 to attain a reasonable probability of being well absorbed. [d] Absorption level; 3 = very low absorption, 2 = low absorption, 1 = moderate, 0 = good absorption. [e] Blood–brain barrier level; 4 = undefined, 3 = low penetration 2 = medium penetration, 1 = high penetration.

the co-crystallized ligand (**VII**) was redocked, and the docked pose showed RMSD value of 0.5446 Å when aligned to the X-ray geometry (the co-crystallized bioactive conformation) (Fig. 3) confirming the validation of the used protocol in expecting the pose of the inhibitors in the X-ray structure of PI3K-α.

Docking 6-methylfuro[2,3-*d*]pyrimidines of the target compounds revealed that derivatives (**7a**, **d**) and (**8b–c**) fulfilled the basic key interactions of PI3K-α inhibitors, where the oxygen atom of furan ring forms a H-bond with Val851 at the hinge region and the and another hydrogen bond is formed with the catalytic Lys802 through the oxygen atom of either the aryloxyacetyl or urea series. The ester moiety saturated the ribose pocket by hydrophobic interaction with different residues whether with Ser854, or Gln859. Compounds with amide linkage (5a–d) missed the key interaction with Lys802 residue, resulting in lower docking scores. These results may also deduce their PI3K inhibitory inactivity in the kinase assay.

Interestingly, compound (**7b**) showed a flipped orientation, preserving the required key interaction in a different approach. The thiomethyl moiety formed a hydrogen bond with the Val851 residue instead of the furopyrimidine's oxygen atom and the NCO moiety formed a hydrogen bond with the catalytic Lys802 amino acid while the furopyrimidine ring bound to the ribose pocket. Although compound (**7c**), the aryloxyacetyl derivative, was expected to show similar inhibitory activity, yet the docking study shown that the *tert*-butyl group led to repositioning of the furopyrimidine core, which prevented it from binding to the hinge region, and the NCO group formed the hydrogen bond with Val851 instead, moreover, it missed the key hydrogen bonding with Lys802, explaining the loss of inhibitory activity of this compound (Fig. 4).

The urea derivative (**8a**) (PI3K-α inhibition; 69%) established highest docking scores within all the target compounds. Yet, it performed a slightly different orientation, where the terminal aromatic ring formed a pi–pi T shaped bond with Trp780 in the specificity pocket.

Conclusion

Novel furo[2,3-*d*]pyrimidine derivatives were designed, synthesized and evaluated for their *in vitro* PI3K-α inhibitory activity and their anti-proliferative activity against the PANC-1 cell line as well as NCI 60 cell line panel. Compounds bearing a urea linker or aryloxyacetyl moieties showed moderate PI3K-α inhibition (45–69%) at 10 μM concentration except for the aryloxyacetyl derivative compound (**7c**) due to its bulky *p-tert*-butyl substituent. The amide-based derivatives (**5a–5d**) showed poor PI3K-α inhibition (0–28%) at 10 μM concentration. In addition, compounds (**7b** and **8a**) displayed good *in vitro* ability to inhibit PANC-1 cell line proliferation with IC_{50} values of 4.5 and 6.0 μM respectively. These outcomes were further clarified using molecular docking studies which revealed the ability of the urea-based derivatives to form a network of key interactions, known to be essential for PI3K-α inhibition. However, their amide-based analogues missed a key interaction with Lys802 residue. Moreover, the introduction of the thiomethyl moiety to the ether based compounds led to repositioning the furo[2,3] pyrimidine ring, maintaining the key interactions characterizing PI3K-α inhibitors.

In silico predictive ADME study for targeted compounds

In order to further examine physicochemical properties of the synthesized compounds, computer-aided ADMET study was implemented by using Accelrys Discovery Studio 2.5 software.

These studies are based on a protocol that calculates a long list of traditional molecular descriptors, semiempirical quantum mechanics (QM) descriptors, density functional QM descriptors, as well as user-built QSAR models. As a result, a prediction various molecular properties can be obtained based on the given molecular chemical structure. Parameters including atom-based log P98 (A log P98), aqueous solubility level (AQ SOl LEV), 2D polar surface area (ADMET 2D PSA), and blood–brain barrier level (BBB LEV), were calculated to expect

compounds pharmacokinetics. Anticipation of the aqueous solubility level was made for the target compounds, showing fluctuating values (2–3) between good and low solubility (Table 3), which are ideal for oral bioavailability.

PSA is another drug bioavailability aspect, in which actively absorbed molecules with PSA > 140 are considered of poor in oral bioavailability. Here in, the synthesized compounds PSA fell within the range 68–107.1, predicting the presence of good passive oral absorption. Furthermore, results are offered as a 2D ADMET plot, drawn using calculated PSA_2D against A log P98 properties. Blood–brain barrier (BBB) and human intestinal absorption (HIA) plots were presented as well. In BBB plot, almost all the synthesized compounds were located between the 99% and 95% ellipses with a low level of BBB penetration, indicating low CNS adverse effects, unlike the HS-173, which is predicted to highly penetrate the BBB. While, in HIA plot, all the target compounds fell within the 99% ellipse, indicating good intestinal absorption with an absorption level 0 (ESI†).

Experimental

Chemistry and analysis

Starting materials and reagents were purchased from Sigma-Aldrich (USA), and Loba Chemie Organics and were used without further purification. Solvents were purchased from Fisher scientific or Sigma-Aldrich and used without further purification. Anhydrous acetone was dried by distillation. Reactions were monitored by analytical thin layer chromatography (TLC), on silica gel 60 F254 that is packed on aluminum sheets, purchased from Merck, and were visualized under UV light (254 nm). Intermediates monitoring was carried out using melting points, or ^{1}H NMR which matched the reference data. Melting points were measured on an electrothermal apparatus in closed capillary tubes using Gallenkamp melting point apparatus and were uncorrected. ^{1}H NMR spectra were recorded on a Bruker 400 MHz spectrometer in δ scale (ppm), using $CDCl_3$ as solvent and TMS as internal standard signal at the Faculty of Pharmacy, Ain-Shams University. Whereas ^{13}C NMR spectra were recorded a 100 MHz. EI-MS spectra were recorded on direct probe controller inlet part to single quadrupole mass analyzer in (Thermo Scientific GCMS) model (ISQ LT) using Thermo X-Calibur software at the regional center for mycology and biotechnology (RCMB) Al-Azhar University. Elemental analyses were performed at the regional center of mycology and biotechnology at Al-Azhar University. Compounds **1**,[35] **2**, **3** (ref. 39) and the chlorophenylacetamide derivatives,[44,45] were prepared according to the reported procedures.

Ethyl 6-methyl-4-(piperazin-1-yl)furo[2,3-*d*]pyrimidine-5-carboxylate (4). To a solution of piperazine (7.5 equiv., 6.45 g, 75 mmol) in isopropanol (100 mL), ethyl 4-chloro-6-methylfuro [2,3-*d*]pyrimidine-5-carboxylate (**3**) (1 equiv., 2.4 g, 10 mmol) was added, followed by heating under reflux for 6 hours. The reaction mixture was vacuum evaporated; chloroform (50 mL) was added to the residue and filtered. The filtrate was washed with brine and dried over anhydrous sodium sulfate, and then the organic solvent was evaporated to give the target compound (**4**) 60.5%, mp: below 40 °C.

^{1}H-NMR ($CDCl_3$-d_1, 400 MHz): δ (ppm) 8.28 (s, 1H, pyrimidine H), 4.28 (q, J = 7.1 Hz, 2H, CH_2CH_3), 3.5 (t, J = 5 Hz, 4H, piperazine H), 2.86 (t, J = 5 Hz, 4H, piperazine H), 2.57 (s, 3H, CH_3), 2.35 (s, 1H, NH D_2O exchangeable), 1.31 (t, J = 7.1 Hz, 3H, CH_2CH_3); FT-IR (ύ max, cm^{-1}) 3419 (NH), 2956 (C–H aliphatic), 2921 (C–H aromatic), 1719 (C=O), 1589 (C=C).

Ethyl 4-(4-(2-((4-substituted phenyl)amino)-2-oxoethyl) piperazin-1-yl)-6-methylfuro[2,3-*d*]pyrimidine-5-carboxylate (5a–d)

General procedure. To a solution of ethyl 6-methyl-4-(piperazin-1-yl)furo[2,3-*d*]pyrimidine-5-carboxylate (**4**) (1 equiv., 0.283 g, 0.97 mmol), potassium carbonate (4.5 equiv., 0.604 g, 4.37 mmol) and potassium iodide (4.5 equiv., 0.72 g, 4.37 mmol) were added and appropriate 2-chloro-*N*-phenylacetamide derivatives (1 equiv., 0.97 mmol) in acetone (30 mL). The reaction was refluxed for 30–36 h and monitored using TLC (DCM : AcOEt = 1 : 1).

The mixture was vacuum filtered and poured on water (50 mL), filtered then recrystallized from absolute ethanol.

Ethyl 6-methyl-4-(4-(2-oxo-2-(phenylamino)ethyl)piperazin-1-yl)furo[2,3-*d*]pyrimidine-5-carboxylate (5a). The titled compound was separated as buff crystals (41%); mp 140 °C; ^{1}H-NMR ($CDCl_3$-d_1, 400 MHz): δ (ppm) 9.09 (s, 1H, NH D_2O exchangeable), 8.42 (s, 1H, pyrimidine H), 7.58 (d, J = 7.8 Hz, 2H, ArH), 7.36 (t, J = 7.7 Hz, 2H, ArH), 7.14 (t, J = 7.3 Hz, 1H, ArH), 4.40 (q, J = 7.0 Hz, 2H, CH_2CH_3), 3.68 (broad s, 4H, piperazine), 3.20 (s, 2H, $COCH_2$), 2.74 (broad s, 4H, piperazine H), 2.69 (s, 3H, CH_3), 1.42 (t, J = 7.1 Hz, 3H, CH_2CH_3); ^{13}C NMR ($CDCl_3$-d_1, 100 MHz): δ (ppm) 167.9, 167.0, 163.4, 159.5, 158.2, 152.7, 137.4, 129.1 (2C), 124.4, 119.5 (2C), 109.1, 100.4, 62.1, 61.4, 53.1 (2C), 48.57 (2C), 14.4, 14.3; FT-IR (ύ max, cm^{-1}) 3319 (NH), 3065 (C–H aromatic), 2943 (C–H aliphatic), 1686 (C=O), 1591 (C=C); MS: (M_w: 423): m/z, 423 [M$^+$, (23.6%)] 323.4 (100%); anal. calcd for $C_{22}H_{25}N_5O_4$: C, 62.40; H, 5.95; N, 16.54; found: C, 62.31; H, 5.74; N, 16.71.

Ethyl 6-methyl-4-(4-(2-oxo-2-(*p*-tolylamino)ethyl)piperazin-1-yl)furo[2,3-*d*]pyrimidine-5-carboxylate (5b). The titled compound was separated as yellowish white crystals (49%); mp 184 °C; ^{1}H-NMR ($CDCl_3$-d_1, 400 MHz): δ (ppm) 9.01 (s, 1H, NH D_2O exchangeable), 8.41 (s, 1H, pyrimidine H), 7.46 (d, J = 8.2 Hz, 2H, ArH), 7.15 (d, J = 8.1 Hz, 2H, ArH), 4.39 (q, J = 7.1 Hz, 2H, CH_2CH_3), 3.67 (broad s, 4H, piperazine H), 3.18 (s, 2H, $COCH_2$), 2.72 (broad s, 4H, piperazine H), 2.68 (s, 3H, CH_3), 2.33 (s, 3H, Ar CH_3), 1.42 (t, J = 7.1 Hz, 3H, CH_2CH_3); ^{13}C NMR ($CDCl_3$-d_1, 100 MHz): δ (ppm) 167.7, 167.0, 163.4, 159.5, 158.1, 152.7, 134.9, 134.0, 129.6 (2C), 119.49 (2C), 109.13, 101.31, 62.06, 61.38, 53.0 (2C), 48.6 (2C), 20.9, 14.4, 14.3; FT-IR (ύ max, cm^{-1}) 3298 (NH), 3030 (C–H aromatic), 2918 (C–H aliphatic), 1674 (C=O), 1593 (C=C); MS: (M_w: 437): m/z, 457 [M$^+$, (20.87%)] 329.09 (100%); anal. calcd for $C_{23}H_{27}N_5O_4$: C, 63.14; H, 6.22; N, 16.01; found: C, 63.14; H, 6.20; N, 16.01.

Ethyl 4-(4-(2-((4-methoxyphenyl)amino)-2-oxoethyl)piperazin-1-yl)-6-methylfuro[2,3-*d*]pyrimidine-5-carboxylate (5c). The titled compound was separated as reddish white crystals (38%); mp 131 °C; ^{1}H-NMR ($CDCl_3$-d_1, 400 MHz): δ (ppm) 8.96 (s, 1H, NH D_2O exchangeable), 8.41 (s, 1H, pyrimidine H), 7.48 (d, J = 8.8 Hz, 2H, ArH), 6.88 (d, J = 8.8 Hz, 2H, ArH), 4.38 (q, J =

7.0 Hz, 2H, CH_2CH_3), 3.80 (s, 3H, OCH_3), 3.67 (broad s, 4H, piperazine H), 3.18 (s, 2H, $COCH_2$), 2.72 (broad s, 4H, piperazine H), 2.68 (s, 3H, CH_3), 1.41 (t, J = 7.1 Hz, 3H, CH_2CH_3); ^{13}C NMR ($CDCl_3$-d_1, 100 MHz): δ (ppm) 167.6, 167.0, 163.4, 159.5, 158.1, 156.4, 152.7, 130.7, 121.2 (2C), 114.2 (2C), 109.13, 101.3, 62.0, 61.4, 55.5, 53.1 (2C), 48.6 (2C), 14.4, 14.3; FT-IR ($\dot{\upsilon}$ max, cm^{-1}) 3281 (NH), 3040 (C–H aromatic), 2916 (C–H aliphatic), 1682 (C=O), 1593 (C=C); MS: (M_w: 451): m/z, 451 [M^+, (22.4%)] 329 (100%); anal. calcd for $C_{23}H_{27}N_5O_5$: C, 60.92; H, 6.00; N, 15.44; found: C, 60.92; H, 5.93; N, 15.41.

Ethyl 4-(4-(2-((4-chlorophenyl)amino)-2-oxoethyl)piperazin-1-yl)-6-methylfuro[2,3-*d*]pyrimidine-5-carboxylate (5d). The titled compound was separated as white crystals (84%); mp 160 °C; ^{1}H-NMR ($CDCl_3$-d_1, 400 MHz): δ (ppm) 9.24 (s, 1H, NH D_2O exchangeable), 8.42 (s, 1H, pyrimidine H), 7.55 (d, J = 8.4 Hz, 2H, ArH), 7.30 (d, J = 8.4 Hz, 2H, ArH), 4.39 (q, J = 7.0 Hz, 2H, CH_2CH_3), 3.69 (broad s, 4H, piperazine H), 3.26 (s, 2H, $COCH_2$), 2.80 (broad s, 4H, piperazine H), 2.69 (s, 3H, CH_3), 1.42 (t, J = 7.0 Hz, 3H, CH_2CH_3); ^{13}C NMR ($CDCl_3$-d_1, 100 MHz): δ (ppm) 167.0 (2C), 163.4, 159.5, 158.4, 152.7, 136.1, 129.3, 129.1 (2C), 120.7 (2C), 109.0, 101.5, 61.8, 61.4, 53.0 (2C), 48.3 (2C), 14.4 (2C); FT-IR ($\dot{\upsilon}$ max, cm^{-1}) 3300 (NH), 3036 (C–H aromatic), 2934 (C–H aliphatic), 1693 (C=O), 1589 (C=C). MS: (M_w: 457): m/z, 457 [M^+, (21.27%)] 285.57 (100%); anal. calcd for $C_{22}H_{24}ClN_5O_4$: C, 57.71; H, 5.28; N, 15.29; found: C, 57.89; H, 5.48; N, 15.57.

Ethyl 4-(4-(2-chloroacetyl)piperazin-1-yl)-6-methylfuro[2,3-*d*]pyrimidine-5-carboxylate (6). To a solution of ethyl 6-methyl-4-(piperazin-1-yl)furo[2,3-*d*]pyrimidine-5-carboxylate (**4**) (1 equiv., 1 g, 3.4 mmol) in (20 mL) chloroform, chloroacetyl chloride (3.1 equiv., 1.2 g, 10.6 mmol) was added portion wise at 0 °C in an ice bath and stirred for 3 h. Triethylamine (1 mL, 7.5 mmol) was then added as a base. The completion of the reaction was monitored by TLC. The reaction mixture was then, vacuum evaporated and washed with ice/ammonia (33%, 5 mL). White crystals were formed and filtered to give the titled compound (**6**) (62%), mp; 128 °C, which was then used in the next step without further purification; ^{1}H-NMR ($CDCl_3$-d_1, 400 MHz): δ (ppm) 8.44 (s, 1H, pyrimidine H), 4.39 (q, J = 7.1, 2H, CH_2CH_3), 4.12 (s, 2H, $COCH_2$), 3.96–3.26 (m, 8H, piperazine H), 2.71 (s, 3H, CH_3), 1.42 (t, J = 7.1, 3H, CH_2CH_3); FT-IR ($\dot{\upsilon}$ max, cm^{-1}) 3059 (C–H aromatic), 2938 (C–H aliphatic), 1643 (C=O), 1593 (C=C); MS: (M_w: 366): m/z, 366 [M^+, (44.09%)] 330 (100%); anal. calcd for $C_{16}H_{19}ClN_4O_4$: C, 52.39; H, 5.22; N, 15.27; found: C, 52.47; H, 5.38; N, 15.13.

Ethyl 4-(4-(2-(substituted phenoxy)acetyl)piperazin-1-yl)-6-methylfuro[2,3-*d*]pyrimidine-5-carboxylate (7a–d)

General procedure. To a solution of ethyl 4-(4-(2-chloroacetyl) piperazin-1-yl)-6-methylfuro[2,3-*d*]pyrimidine-5-carboxylate (**6**) in (30 mL) acetone, potassium carbonate (4.5 equiv., 0.604 g, 4.37 mmol) and potassium iodide (4.5 equiv., 0.72 g, 4.37 mmol) were added (1 equiv., 0.283 g, 0.97 mmol) along with appropriate phenolic derivatives (3,4-dichlorophenol, 4-(methylthio) phenol, 4-*tert*-butylphenol, and phenol) (1 equiv., 0.97 mmol) in acetone 30 mL. The reaction was refluxed for 20–30 h and monitored using TLC (DCM : AcOEt = 1 : 1). The mixture was vacuum evaporated and poured on water, filtered then recrystallized from absolute ethanol.

Ethyl 6-methyl-4-(4-(2-phenoxyacetyl)piperazin-1-yl)furo[2,3-*d*]pyrimidine-5-carboxylate (7a). The titled compound was separated as pale white crystals (57%); mp 120 °C; ^{1}H-NMR ($CDCl_3$-d_1, 400 MHz): δ (ppm) 8.43 (s, 1H, pyrimidine H), 7.32 (t, J = 8.0 Hz, 2H, ArH), 7.08–6.9 (m, 3H, ArH), 4.75 (s, 2H, $COCH_2$),4.38 (q, J = 6.4, 2H, CH_2CH_3), 3.92–3.51 (m, 8H, piperazine H), 2.70 (s, 3H, CH_3), 1.39 (t, J = 6.7, 3H, CH_2CH_3); ^{13}C NMR ($CDCl_3$-d_1, 100 MHz): δ (ppm) 166.8 (2C), 163.3, 158.7, 157.7, 152.4 (2C), 129.7 (2C), 121.9, 114.5 (2C), 109.0, 101.6, 67.9, 61.5, 48.9, 48.5, 45.1, 41.8, 14.4, 14.3; FT-IR ($\dot{\upsilon}$ max, cm^{-1}) 3053 (C–H aromatic), 2932 (C–H aliphatic), 1657 (C=O),1587 (C=C); MS: (M_w: 424): m/z, 424 [M^+, (29.74%)] 285.79 (100%); anal. calcd for $C_{22}H_{24}N_4O_5$: C, 62.25; H, 5.70; N, 13.20; found: C, 62.57; H, 5.82; N, 13.47.

Ethyl 6-methyl-4-(4-(2-(4-(methylthio)phenoxy)acetyl)piperazin-1-yl)furo[2,3-*d*]pyrimidine-5-carboxylate (7b). The titled compound was separated as yellowish white crystals (29%); mp 119 °C; ^{1}H-NMR ($CDCl_3$-d_1, 400 MHz): δ (ppm) 8.43 (s, 1H, pyrimidine H), 7.27 (d, J = 8.8 Hz, 2H, ArH), 6.92 (d, J = 8.6 Hz, 2H, ArH), 4.73 (s, 2H, $COCH_2$), 4.37 (q, J = 7, 2H, CH_2CH_3), 3.80–3.47 (m, 8H, piperazine H), 2.7 (s, 3H, SCH_3), 2.46 (s, 3H, CH_3), 1.4 (t, J = 7.1, 3H, CH_2CH_3); ^{13}C NMR ($CDCl_3$-d_1, 100 MHz): δ (ppm) 166.9, 166.6, 163.3, 159.3, 158.6, 156.1, 152.6, 130.4, 129.8 (2C), 115.3 (2C), 109.0, 101.6, 68.0, 61.5, 48.8, 48.4, 45.1, 41.8, 17.6, 14.4, 14.3; FT-IR ($\dot{\upsilon}$ max, cm^{-1}) 3028 (C–H aromatic), 2901 (C–H aliphatic), 1645 (C=O), 1591 (C=C); MS: (M_w: 470): m/z, 470 [M^+, (14%)] 316.87 (100%); anal. calcd for $C_{23}H_{26}N_4O_5S$: C, 58.71; H, 5.57; N, 11.91; found: C, 58.45; H, 5.79; N, 11.82.

Ethyl 4-(4-(2-(4-(*tert*-butyl)phenoxy)acetyl)piperazin-1-yl)-6-methylfuro[2,3-*d*]pyrimidine-5-carboxylate (7c). The titled compound was separated as white crystals (30%); mp 140 °C; ^{1}H-NMR ($CDCl_3$-d_1, 400 MHz): δ (ppm) 8.47 (s, 1H, pyrimidine H), 7.33 (d, J = 8.8 Hz, 2H, ArH), 6.91 (d, J = 8.8 Hz, 2H, ArH), 4.73 (s, 2H, $COCH_2$),4.39 (q, J = 7.2, 2H, CH_2CH_3), 3.87–3.5 (m, 8H, piperazine H), 2.72 (s, 3H, CH_3), 1.41 (t, J = 7.1, 3H, CH_2CH_3), 1.31 (s, 9H, $(CH_3)_3$); ^{13}C NMR ($CDCl_3$-d_1, 100 MHz): δ (ppm) 166.9 (2C), 163.3, 159.4, 158.4, 155.4, 152.6, 144.5, 126.4 (2C), 113.99 (2C), 108.98, 101.50, 67.90, 61.39, 48.67, 48.38, 45.08, 41.75, 34.10, 31.46 (3C), 14.32 (2C); FT-IR ($\dot{\upsilon}$ max, cm^{-1}) 3047 (C–H aromatic), 2964 (C–H aliphatic), 1661 (C=O),1585 (C=C); MS: (M_w: 480): m/z, 480 [M^+, (11.9%)] 375.2 (100%); anal. calcd for $C_{26}H_{32}N_4O_5$: C, 64.98; H, 6.71; N, 11.66; found: C, 64.89; H, 6.58; N, 11.59.

Ethyl 4-(4-(2-(3,4-dichlorophenoxy)acetyl)piperazin-1-yl)-6-methylfuro[2,3-*d*]pyrimidine-5-carboxylate (7d). The titled compound was separated as buff crystals (60%); mp 148 °C; ^{1}H-NMR ($CDCl_3$-d_1, 400 MHz): δ (ppm) 8.41 (s, 1H, pyrimidine H), 7.33 (d, J = 8.9 Hz, 1H, ArH), 7.06 (s, 1H, ArH), 6.83 (dd, J = 8.8, 2.5 Hz, 1H, ArH), 4.72 (s, 2H, $COCH_2$), 4.37 (q, J = 7.0 Hz, 2H, CH_2CH_3), 3.84–3.37 (m, 8H, piperazine H), 2.69 (s, 3H, CH_3), 1.39 (t, J = 7.1 Hz, 3H, CH_2CH_3); ^{13}C NMR ($CDCl_3$-d_1, 100 MHz): δ (ppm) 166.9, 165.8, 163.3, 159.5, 158.7, 156.8, 152.7, 133.1, 130.9, 125.2, 116.8, 114.4, 108.9, 101.7, 67.8, 61.4, 48.8, 48.3, 44.9, 41.8, 14.4, 14.3; FT-IR ($\dot{\upsilon}$ max, cm^{-1}) 3031 (C–H aromatic), 2933 (C–H aliphatic), 1666 (C=O), 1590 (C=C); MS: (M_w: 492): m/z, 492 [M^+, (23.37%)] 321.18 (100%); anal. calcd for

$C_{22}H_{22}Cl_2N_4O_5$: C, 53.56; H, 4.49; N, 11.36; found: C, 53.56; H, 4.79; N, 11.36.

Ethyl 6-methyl-4-(4-(substitutedcarbamoyl)piperazin-1-yl) furo[2,3-*d*]pyrimidine-5-carboxylate and ethyl 6-methyl-4-(4-(phenylcarbamothioyl)piperazin-1-yl)furo[2,3-*d*]pyrimidine-5-carboxylate (8a–c)

General procedure. To a solution of ethyl 6-methyl-4-(piperazin-1-yl)furo[2,3-*d*]pyrimidine-5-carboxylate (**4**) (1 equiv., 0.2 g, 0.69 mmol) in chloroform (40 mL), the respective aryl isocyanate or aryl isothiocyanate (1 equiv., 0.69 mmol) were added and stirred for 6 h at room temperature. The chloroform was vacuum evaporated and the precipitate was recrystallized from ethanol.

Ethyl 6-methyl-4-(4-(phenylcarbamoyl)piperazin-1-yl)furo [2,3-*d*]pyrimidine-5-carboxylate (8a). The titled compound was separated as white crystals (38%); mp 208 °C; ^{1}H-NMR ($CDCl_3$-d_1, 400 MHz): δ (ppm) 8.47 (s, 1H, pyrimidine H), 7.40 (d, J = 7.8 Hz, 2H, ArH), 7.31 (t, J = 7.9 Hz, 2H, ArH), 7.07 (t, J = 7.3 Hz, 1H, ArH), 6.62 (s, 1H, NH D_2O exchangeable), 4.41 (q, J = 7.1 Hz, 2H, CH_2CH_3), 3.99–3.39 (m, 8H, piperazine H), 2.72 (s, 3H, CH_3), 1.43 (t, J = 7.1 Hz, 3H, CH_2CH_3); ^{13}C NMR ($CDCl_3$-d_1, 100 MHz): δ (ppm) 166.9, 163.4, 159.4, 158.3, 155.2, 152.6, 138.9, 128.9 (2C), 123.4, 120.3 (2C), 109.1, 101.4, 61.5, 48.2 (2C), 43.7 (2C), 14.4, 14.3; FT-IR (ύ max, cm^{-1}) 3285 (NH), 3040 (C–H aromatic), 2955 (C–H aliphatic), 1632 (C=O), 1591 (C=C); MS: (M_w: 409): m/z, 409 [M^+, (18.95%)] 222.16 (100%); anal. calcd for $C_{21}H_{23}N_5O_{64}$: C, 61.60; H 5.66; N, 17.10; found: C, 61.78; H, 5.89; N, 16.89.

Ethyl 6-methyl-4-(4-(*m*-tolylcarbamoyl)piperazin-1-yl)furo [2,3-*d*]pyrimidine-5-carboxylate (8b). The titled compound was separated as yellow crystals (40%); mp 204 °C; ^{1}H-NMR ($CDCl_3$-d_1, 400 MHz): δ (ppm) 8.46 (s, 1H, pyrimidine H), 7.28 (s, 1H, ArH), 7.23–7.13 (m, 2H, ArH), 6.88 (d, 1H, J = 7.0 Hz, ArH), 6.55 (s, 1H, NH D_2O exchangeable), 4.41 (q, J = 7.1 Hz, 2H, CH_2CH_3), 3.77–3.58 (m, 8H, piperazine H), 2.72 (s, 3H, CH_3), 2.34 (s, 3H, toluene CH_3), 1.43 (t, J = 7.1 Hz, 3H, CH_2CH_3); ^{13}C NMR ($CDCl_3$-d_1, 100 MHz): δ (ppm) 166.7, 163.1, 162.4,157.5, 155.1, 153.7, 138.8, 138.7, 128.7, 120.8, 124.2, 117.1, 110.9, 106.0, 61.7, 48.7 (2C), 43.7 (2C), 21.5, 14.4, 14.3; FT-IR (ύ max, cm^{-1}) 3300 (NH), 3042 (C–H aromatic), 2924 (C–H aliphatic), 1636 (C=O), 1589 (C=C); MS: (M_w: 423): m/z, 423 [M^+, (23.7%)] 419.87 (100%); anal. calcd for $C_{22}H_{25}N_5O_4$: C, 62.40; H, 5.95; N, 16.54; found: C, 62.49; H, 6.14; N, 16.73.

Ethyl 6-methyl-4-(4-(phenylcarbamothioyl)piperazin-1-yl) furo[2,3-*d*]pyrimidine-5-carboxylate (8c). The titled compound was separated as buff crystals (30%); mp 159 °C; ^{1}H-NMR ($CDCl_3$-d_1, 400 MHz): δ (ppm) 8.38 (s, 1H, pyrimidine H), 7.66 (1H, NH D_2O exchangeable) 7.32 (t, J = 7.8, 2H, ArH), 7.18–7.10 (m, 3H, ArH), 4.36 (q, J = 7.1 Hz, 2H, CH_2CH_3), 4.00–3.86 (m, 4H, piperazine H), 3.71–3.60 (m, 4H, piperazine H), 2.67 (s, 3H, CH_3), 1.39 (t, J = 7.1 Hz, 3H, CH_2CH_3); ^{13}C NMR ($CDCl_3$-d_1, 100 MHz): δ (ppm) 183.5, 166.9, 163.4, 159.3, 158.3, 152.6, 139.9, 129.2 (2C), 125.4, 123.3 (2C), 109.0, 101.4, 61.5, 48.8 (2C), 47.7 (2C), 14.3, 14.3; FT-IR (ύ max, cm^{-1}) 3238 (NH), 3044 (C–H aromatic), 2928 (C–H aliphatic), 1618 (C=O), 1587 (C=C), 1231 (C=S); MS: (M_w: 425): m/z, 425 [M^+, (48.18%)] 392.3 (100%); anal. calcd for $C_{21}H_{23}N_5O_3S$: C, 59.28; H, 5.45; N, 16.46; found: C, 59.52; H, 5.63; N, 16.72.

Biological evaluation

PI3K-α inhibitory assay. The *in vitro* enzyme inhibition assay for the synthesized compounds was carried out in Thermo Fisher Scientific, Life Technologies. The PI3K-α activity was performed, where the PIK3CA/PIK3P1 (p110 alpha/p85 alpha) (# 1014) served as the enzyme source, PIP2 : PS served as the standardized substrate and Adapta Universal Kinase Assay Kit was used (ESI†).

***In vitro* anti-proliferative activity assay against NCI 60-cell line panel.** The NCI *in vitro* anticancer screening is a two-stage process, beginning with all compounds assessment against the full NCI 60 cell lines panel representing leukemia, NSCLC, melanoma, colon cancer, CNS cancer, breast cancer, ovarian cancer, renal cancer and prostate cancer at a single dose of 10 mM. The output from the single dose screen is reported as a mean graph (ESI†).

***In vitro* PANC-1 anti-proliferative assay.** The PANC-1 cell line anti-proliferative assay for selected compounds was carried out at Nawah Scientific Inc, (Mokatam, Cairo, Egypt), where the PANC-pancreas/duct epithelioid cells, human (ATCC® CRL1469™) served as the cells' source in ATCC-formulated Dulbecco's modified Eagle's medium, (ATCC # 30-2002). IC_{50} values were determined using sigmoidal concentration response curve fitting models (Sigma plot software) (ESI†).

Molecular docking

Molecular modeling was carried out using C-Docker 2.5 software in the interface of Accelry's Discovery Studio 2.5 (Accelrys Inc., San Diego, CA, USA) at Faculty of Pharmacy, Ain Shams University, drug design laboratory. The X-ray crystal structure of PI3K-α co-crystallized with the imidazopyridine-based compound (**I**) was obtained from the Protein Data Bank at the Research Collaboration for Structural Bioinformatics (RCSB) website [https://www.rcsb.org] (PDB code: 4ZOP) and loaded in Accelry's Discovery (ESI†).

Conflicts of interest

There are no conflicts to declare.

Notes and references

1 F. M. Elmenier, D. S. Lasheen and K. A. M. Abouzid, Phosphatidylinositol 3 kinase (PI3K) inhibitors as new weapon to combat cancer, *Eur. J. Med. Chem.*, 2019, **183**, 111718.
2 S. Jean and A. A. Kiger, Classes of phosphoinositide 3-kinases at a glance, *J. Cell Sci.*, 2014, **127**, 923–928.
3 B. Vanhaesebroeck, J. Guillermet-Guibert, M. Graupera and B. Bilanges, The emerging mechanisms of isoform-specific PI3K signalling, *Nat. Rev. Mol. Cell Biol.*, 2010, **11**, 329–341.

4 C. Sheridan and J. Downward, Inhibiting the RAS-PI3K Pathway in Cancer Therapy, in *Enzymes*, Elsevier Inc., 1st edn, 2013, vol. 34, pp. 107–136.
5 P. Liu, H. Cheng, T. M. Roberts and J. J. Zhao, Targeting the phosphoinositide 3-kinase pathway in cancer, *Nat. Rev. Drug Discovery*, 2009, **8**, 627–644.
6 X. Shi, J. Wang, Y. Lei, C. Cong, D. Tan and X. Zhou, Research progress on the PI3K/AKT signaling pathway in gynecological cancer (review), *Mol. Med. Rep.*, 2019, **19**, 4529–4535.
7 M. Löhr, G. Klöppel, P. Maisonneuve, A. B. Lowenfels and J. Lüttges, Frequency of K-ras mutations in pancreatic intraductal neoplasias associated with pancreatic ductal adenocarcinoma and chronic pancreatitis: a meta-analysis, *Neoplasia*, 2005, **7**, 17–23.
8 R. Baer, C. Cintas, N. Therville and J. Guillermet-Guibert, Implication of PI3K/Akt pathway in pancreatic cancer: when PI3K isoforms matter?, *Adv. Biol. Regul.*, 2015, **59**, 19–35.
9 R. Baer, C. Cintas, M. Dufresne, S. Cassant-Sourdy, N. Schönhuber, L. Planque, H. Lulka, B. Couderc, C. Bousquet, B. Garmy-Susini, B. Vanhaesebroeck, S. Pyronnet, D. Saur and J. Guillermet-Guibert, Pancreatic cell plasticity and cancer initiation induced by oncogenic Kras is completely dependent on wild-type PI 3-kinase p110α, *Genes Dev.*, 2014, **28**, 2621–2635.
10 B. A. Ruggeri, L. Huang, M. Wood, J. Q. Cheng and J. R. Testa, Amplification and Overexpression of the AKT2 Oncogene in a Subset of Human Pancreatic Ductal, *Adenocarcinomas*, 1998, **86**, 81–86.
11 M. G. Schlieman, B. N. Fahy, R. Ramsamooj, L. Beckett and R. J. Bold, Incidence, mechanism and prognostic value of activated AKT in pancreas cancer, *Br. J. Cancer*, 2003, **89**, 2110–2115.
12 F. Bray, J. Ferlay and I. Soerjomataram, Global Cancer Statistics 2018: GLOBOCAN Estimates of Incidence and Mortality Worldwide for 36 Cancers in 185 Countries, *Ca-Cancer J. Clin.*, 2018, 394–424.
13 L. Rahib, B. D. Smith, R. Aizenberg, A. B. Rosenzweig, J. M. Fleshman and L. M. Matrisian, Projecting Cancer Incidence and Deaths to 2030: The Unexpected Burden of Thyroid, Liver, and Pancreas Cancers in the United States, *Cancer Res.*, 2014, DOI: 10.1158/0008-5472.CAN-14-0155.
14 R. L. Siegel, K. D. Miller and A. Jemal, Cancer statistics, 2020, *Ca-Cancer J. Clin.*, 2020, **70**, 7–30.
15 M. Orth, P. Metzger, S. Gerum, J. Mayerle, G. Schneider, C. Belka, M. Schnurr and K. Lauber, Pancreatic ductal adenocarcinoma: biological hallmarks, current status, and future perspectives of combined modality treatment approaches, *Radiat. Oncol.*, 2019, **14**, 141.
16 S. Gillen, T. Schuster, C. Meyer zum Büschenfelde, H. Friess and J. Kleeff, Preoperative/Neoadjuvant Therapy in Pancreatic Cancer: A Systematic Review and Meta-analysis of Response and Resection Percentages, *PLoS Med.*, 2010, **7**, e1000267.
17 H. A. Burris, M. J. Moore, J. Andersen, M. R. Green, M. L. Rothenberg, M. R. Modiano, M. C. Cripps, R. K. Portenoy, A. M. Storniolo, P. Tarassoff, R. Nelson, F. A. Dorr, C. D. Stephens and D. D. Von Hoff, Improvements in survival and clinical benefit with gemcitabine as first-line therapy for patients with advanced pancreas cancer: a randomized trial, *J. Clin. Oncol.*, 1997, **15**, 2403–2413.
18 I. Garrido-Laguna and M. Hidalgo, Pancreatic cancer: from state-of-the-art treatments to promising novel therapies, *Nat. Rev. Clin. Oncol.*, 2015, **12**, 319–334.
19 K. E. Behrns, FOLFIRINOX *versus* Gemcitabine for Metastatic Pancreatic Cancer, *Surgery*, 2011, **364**, 1817–1825.
20 M. Amrutkar and I. P. Gladhaug, Pancreatic Cancer Chemoresistance to Gemcitabine, *Cancers*, 2017, **9**, 157.
21 A. Markham, Alpelisib: First Global Approval, *Drugs*, 2019, **79**, 1249–1253.
22 J. R. W. Conway, D. Herrmann, T. R. J. Evans, J. P. Morton and P. Timpson, Combating pancreatic cancer with PI3K pathway inhibitors in the era of personalised medicine, *Gut*, 2019, **68**, 742–758.
23 P. Furet, V. Guagnano, R. A. Fairhurst, P. Imbach-weese, I. Bruce, M. Knapp, C. Fritsch, F. Blasco, J. Blanz, R. Aichholz, J. Hamon, D. Fabbro and G. Caravatti, Discovery of NVP-BYL719 a potent and selective phosphatidylinositol-3 kinase alpha inhibitor selected for clinical evaluation, *Bioorg. Med. Chem. Lett.*, 2013, **23**, 3741–3748.
24 O. Kim, Y. Jeong, H. Lee, S.-S. Hong and S. Hong, Design and Synthesis of Imidazopyridine Analogues as Inhibitors of Phosphoinositide 3-Kinase Signaling and Angiogenesis, *J. Med. Chem.*, 2011, **54**, 2455–2466.
25 M. Rumman, K. H. Jung, Z. Fang, H. H. Yan, M. K. Son, S. J. Kim, J. Kim, J. H. Park, J. H. Lim, S. Hong and S.-S. Hong, HS-173, a novel PI3K inhibitor suppresses EMT and metastasis in pancreatic cancer, *Oncotarget*, 2016, **7**, 78029–78047.
26 P. Wu and Y. Hu, Small molecules targeting phosphoinositide 3-kinases, *Medchemcomm*, 2012, **3**, 1337–1355.
27 S. Maheshwari, M. S. Miller, R. O'Meally, R. N. Cole, L. M. Amzel and S. B. Gabelli, Kinetic and structural analyses reveal residues in phosphoinositide 3-kinase α that are critical for catalysis and substrate recognition, *J. Biol. Chem.*, 2017, **292**, 13541–13550.
28 Y. Liu, W.-Z. Wan, Y. Li, G.-L. Zhou and X.-G. Liu, Recent development of ATP-competitive small molecule phosphatidylinostitol-3-kinase inhibitors as anticancer agents, *Oncotarget*, 2017, **8**, 7181–7200.
29 M. S. Miller, P. E. Thompson and S. B. Gabelli, Structural determinants of isoform selectivity in pi3k inhibitors, *Biomolecules*, 2019, **9**, 1–34.
30 M. A. Aziz, R. A. T. Serya, D. S. Lasheen and K. A. M. Abouzid, Furo[2,3-*d*]pyrimidine based derivatives as kinase inhibitors and anticancer agents, *Future J. Pharm. Sci.*, 2016, **2**, 1–8.
31 R. S. Viswas, S. Pundir and H. Lee, Design and synthesis of 4-piperazinyl quinoline derived urea/thioureas for anti-breast cancer activity by a hybrid pharmacophore approach, *J. Enzyme Inhib. Med. Chem.*, 2019, **34**, 620–630.

32 H. M. Shallal and W. A. Russu, Discovery, synthesis, and investigation of the antitumor activity of novel piperazinylpyrimidine derivatives, *Eur. J. Med. Chem.*, 2011, **46**, 2043–2057.

33 S. Ponnurangam, D. Standing, P. Rangarajan and D. Subramaniam, Tandutinib inhibits the Akt/mTOR signaling pathway to inhibit colon cancer growth, *Mol. Cancer Ther.*, 2013, **12**, 598–609.

34 C. M. Dehnhardt, A. M. Venkatesan, E. Delos Santos, Z. Chen, O. Santos, S. Ayral-Kaloustian, N. Brooijmans, R. Mallon, I. Hollander, L. Feldberg, J. Lucas, I. Chaudhary, K. Yu, J. Gibbons, R. Abraham and T. S. Mansour, Lead optimization of *N*-3-substituted 7-morpholinotriazolopyrimidines as dual phosphoinositide 3-kinase/mammalian target of rapamycin inhibitors: discovery of PKI-402, *J. Med. Chem.*, 2010, **53**, 798–810.

35 M. Bakavoli, B. Feizyzadeh and M. Rahimizadeh, Investigation of hydrazine addition to functionalized furans: synthesis of new functionalized 4,4′-bipyrazole derivatives, *Tetrahedron Lett.*, 2006, **47**, 8965–8968.

36 M. A. Aziz, R. A. T. Serya, D. S. Lasheen, A. K. Abdel-Aziz, A. Esmat, A. M. Mansour, A. N. B. Singab and K. A. M. Abouzid, Discovery of Potent VEGFR-2 Inhibitors based on Furopyrimidine and Thienopyrimidne Scaffolds as Cancer Targeting Agents, *Sci. Rep.*, 2016, **6**, 24460.

37 K. Matsuno, Y. Nomoto, M. Ichimura, S. Ide and S. Oda, Nitrogenous heterocyclic compounds, *US Pat.*, US6423716, 2000.

38 I. Bharatam and Chakraborti Group, *Mono-Alkylation of a Phenol with 1,2-Dibromoethane via Williamson Ether Synthesis; Substituted Phenolic Ether*, National Institute of Pharmaceutical Education and Research, http://cssp.chemspider.com/Article.aspx?id=253.

39 B. Li, W. Gao-wei, Z. Xiao-juan and G. Wen-xian, Synthesis of 2-phenyl-(4-pyrrolidinylethoxyphenyl)ethan-1-one, *Chem. Res. Appl.*, 2012, **24**, 936–939.

40 H. H. Fahmy, A. El-masry and S. H. Ali Abdelwahed, Synthesis and Preliminary Antimicrobial Screening of New Benzimidazole Heterocycles, *Arch. Pharmacal Res.*, 2001, **24**, 27–34.

41 P. Wipf and R. J. Halter, Chemistry and biology of wortmannin, *Org. Biomol. Chem.*, 2005, **3**, 2053–2061.

42 R. Gradiz, H. C. Silva, L. Carvalho, M. F. Botelho and A. Mota-Pinto, MIA PaCa-2 and PANC-1 - pancreas ductal adenocarcinoma cell lines with neuroendocrine differentiation and somatostatin receptors, *Sci. Rep.*, 2016, **6**, 1–14.

43 R. H. Shoemaker, The NCI60 human tumour cell line anticancer drug screen, *Nat. Rev. Cancer*, 2006, **6**, 813–823.

44 D. C. P. Singh, S. R. Hashim and R. G. Singhal, Synthesis and antimicrobial activity of some new thioether derivatives of quinoxaline, *E-J. Chem.*, 2011, **8**, 635–642.

45 S. A. Katke, S. V Amrutkar, R. J. Bhor and M. V Khairnar, Synthesis of Biologically Active 2-Chloro-*N*-Alkyl/Aryl Acetamide Derivatives, *Int. J. Pharma Sci. Res.*, 2011, **2**, 148–156.

